Investigation of the cAMP Receptor Protein Secondary Structure by Raman Spectroscopy

Henry DeGrazia,[‡] James G. Harman,[§] Guo-sheng Tan,[‡] and Roger M. Wartell*,[‡]

Schools of Physics and Biology, Georgia Institute of Technology, Atlanta, Georgia 30332, and Department of Chemistry and Biochemistry, Texas Tech University, Lubbock, Texas 79409

Received August 11, 1989; Revised Manuscript Received November 27, 1989

ABSTRACT: Raman spectroscopy was employed to examine the secondary structure of the cAMP receptor protein (CRP). Spectra were obtained over the range 400–1900 cm^{-1} from solutions of CRP and from CRP–cAMP cocrystals. The spectra of CRP dissolved in 30 mM sodium phosphate and 0.15 M NaCl buffered at either pH 6 or pH 8 or dissolved in 0.15–0.2 M NaCl at protein concentrations of 5, 15, and 30 mg/mL were examined. Estimates of the secondary structure distribution were made by analyzing the amide I region of the spectra (1630–1700 cm^{-1}). CRP secondary structure distributions were essentially the same in either pH and at all protein concentrations examined. The amide I analyses indicated a structural distribution of 44% α-helix, 28% β-strand, 18% turn, and 10% undefined for CRP in solution. Raman spectra of CRP–cAMP cocrystals differed from the spectra of CRP in solution. Some differences were assigned to interfering background bands, whereas other spectral differences were attributed to changes in CRP structure. Differences in the amide III region and in the intensity at 935 cm^{-1} were consistent with alterations in secondary structure. Analysis of the amide I region of the CRP–cAMP cocrystal spectrum indicated a secondary structure distribution of 37% α-helix, 33% β-strand, 17% turn, and 12% undefined. This result is in agreement with a published secondary structure distribution derived from X-ray analysis of CRP–cAMP cocrystals (37% α-helix and 36% β-strand). The Raman data are consistent with a proposal that two bound cAMP induce a shift in CRP secondary structure that includes the conversion of α-helix to β-strand. Other interpretations of the results are discussed.

Cyclic adenosine monophosphate (cAMP) controls transcription from a large number of operons in *Escherichia coli* (Adhya & Garges, 1982; deCrombrugghe et al., 1984; Ullmann & Danchin, 1983). Most known effects of cAMP are mediated by the cAMP receptor protein (CRP), also known as the catabolite gene activator protein (CAP). CRP is isolated as a dimer of two identical polypeptides, each 23 619 Da (Anderson et al., 1971; Aiba et al., 1982; Cossart et al., 1982). In the absence of cAMP, CRP binds DNA nonspecifically. When cAMP forms a complex with CRP, CRP–cAMP binds to specific DNA sequences. This switch in DNA binding specificity is thought to result from a cAMP-induced conformational change in CRP. Evidence for this view comes from a variety of experiments. The fluorescence of a fluorophore attached to CRP is altered upon cAMP binding (Wu et al., 1974). CRP is sensitive to proteases in the presence but not the absence of cAMP (Krakow & Pastan, 1973; Eilen et al., 1978; Harman et al., 1986). Cross-linking studies (Pampeno & Krakow, 1979) and small-angle X-ray scattering (Kumar et al., 1980) indicate a cAMP-induced conformational change in CRP.

A CRP–cAMP complex has been crystallized and its structure determined (McKay et al., 1982; Weber & Steitz, 1987). In this crystalline complex each polypeptide subunit is folded into two domains separated by an eight amino acid "hinge" (Figure 1). The carboxy-terminal domain of each subunit, consisting of amino acid residues 138–209, displays extensive α-helix structure and forms half of the DNA binding surface of the protein. The amino-terminal domain, consisting of amino acid residues 1–129, has extensive β-strand structure and contains the cAMP binding site. Two cAMP molecules are bound to each CRP dimer.

Detailed structural information is lacking for the unliganded form of CRP. Neither the nature of the cAMP-mediated change in CRP structure nor its magnitude is known. McKay et al. (1982) proposed that cAMP may alter the orientation of the two subunits or change the orientation of the domains within a subunit. Gargas and Adhya (1985) presented a related proposal to account for the mutational activation of some cAMP-independent forms of CRP.

Kypr and Mrazek (1985) proposed a structural model of how cAMP binding may influence CRP. This proposal was based on a comparison of the crystalline CRP–cAMP structure with an empirical prediction of CRP secondary structure from its amino acid sequence. Their algorithm correctly predicted 65% of the residues in the carboxy-terminal domain yet was only 23% successful in the amino-terminal domain. In the cAMP binding pocket α-helices were predicted where β-strands are observed. The authors suggested that cAMP binding affects CRP structure, at least in part, by changing an α-helical region to the β-strand segments. Although secondary structure prediction is not by itself highly reliable, evidence exists that some protein regions can switch between α-helix and β-strand conformations depending on the environment (Rosenblatt et al., 1980).

In this study Raman spectroscopy was employed to examine the conformation of CRP. The effect of solvent pH on the CRP spectrum was examined. Spectra of CRP at pH 6 and pH 8 showed no significant differences in vibrational bands sensitive to secondary structure or side-chain environments. The spectrum of CRP in solution was compared to the spectrum from CRP–cAMP cocrystals. Spectral differences observed between these two forms are consistent with the hypothesis that CRP in solution has a higher α-helix content and

* To whom correspondence should be addressed.
‡ Georgia Institute of Technology.
§ Texas Tech University.

0006-2960/90/0429-3557$02.50/0

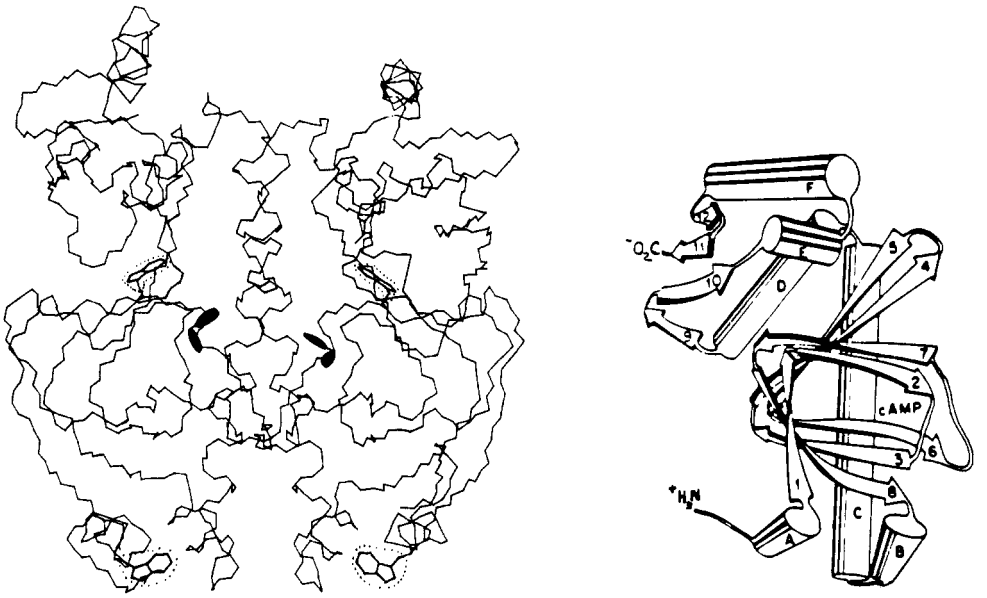

FIGURE 1: (Left) Skeletal polypeptide backbone of the CRP dimer (McKay et al., 1982). The cAMP molecules are indicated as filled-in ellipses. The four tryptophans are enclosed by dotted rings. DNA-binding F α-helices are at the top. (Right) Schematic diagram of CRP monomer from McKay et al. (1982). α-Helices are represented by cylinders A–F and the β-strands by arrows 1–12. The amino-terminal domain contains α-helices A–C and β-strands 1–8. The carboxy-terminal domain contains α-helices D–F and β-strands 9–12.

lower β-strand content than the CRP–cAMP cocrystal complex.

Materials and Methods

CRP was isolated and purified as previously described (DeGrazia et al., 1985; Harman et al., 1986). Protein was isolated on two separate occasions from two different *E. coli* strains. One maintained *crp* on plasmid pHA7 (AMP^r) where *crp* mRNA synthesis originates from the P_{tet} promoter (Aiba et al., 1982). The second maintained two plasmids: pCRP-1 (AMP^r), where *crp* mRNA synthesis originates from the bacteriophage λP_L promoter, and pRK248cI^{ts} (TET^r) (Harman et al., 1986). The latter plasmid encodes a temperature-sensitive bacteriophage λcI repressor. A temperature shift from 30 to 42 °C was used to inactivate cI repressor and promote CRP synthesis. Electrophoretic analysis of protein samples in a 12% polyacrylamide gel with 0.1% SDS indicated purities of 96–98% on the basis of Commassie blue stain. CRP samples were 25–30% active for site-specific binding to the *lac* CRP site (Garner & Revzin, 1981; Fried & Crothers, 1981). Lysozyme and ribonuclease employed in this study as control samples were obtained from Sigma Chemical Co. and dialyzed into the appropriate buffer prior to use.

CRP samples were concentrated in two stages. First, protein solutions were dialyzed to the desired solvent and concentrated to a volume of 50–100 μL on a Centricon-30 filter unit (Millipore Inc.). Losses on the order of 25% were incurred due to protein aggregation, which accumulated on the filter surface. These aggregates were removed by centrifugation at 10000 rpm for 10 min. Samples were further concentrated by centrifugation in a Speedvac (Savant Inc) under a weak vacuum. Final sample volumes of approximately 20 μL were obtained with minimal further loss of active protein (5%). Losses appeared to occur when protein adhered to the sides of tubes and denatured at the liquid–air interface as the fluid receded. Final CRP concentrations ranged from 5 to 30 mg/mL.

Raman spectra were generated with the 5145-Å laser line from an argon ion laser. The instrumentation employed has been described elsewhere (Wartell & Harrell, 1986). At least four separate spectra were obtained for each CRP sample. Each full spectrum (400–1900 cm^{-1}) consisted of four scans recorded at 1-cm^{-1} intervals with a 2-s integration time. The amide I analyses were carried out on spectra consisting of 10–25 scans/spectrum obtained between 1400 and 1800 cm^{-1}. Solution spectra were obtained from samples placed in a 2 mm i.d. quartz capillary cell with a quartz window or from samples placed in melting point capillary tubes. The laser power employed was in the range 120–150 mW. Spectra were collected at a sample temperature of 25 °C. Spectra obtained from two different protein preparations were the same.

Cocrystals of CRP–cAMP were obtained according to the method of McKay and Fried (1983). A 3 mg/mL protein solution was dialyzed at 25 °C into solvent that contained 50 mM potassium phosphate (pH 8.0), 0.1 mM dithiothreitol, 0.1 mM NaN_3, 0.1 mM EDTA, and cAMP at 0.5 mM. Crystals formed overnight. They were packed into a melting point capillary tube by centrifugation for 2 min. The crystals and fresh crystallization solvent were sealed in the capillary tube and placed in a thermally regulated holder. Raman spectra were obtained by scattering defocused laser light off the front surface of the microcrystalline mass with an angle of incidence of about 70° normal to the surface. The temperature of the capillary tube was maintained at 12 or 25 °C. The laser power was between 120 and 200 mW.

Protein secondary structure was evaluated by the analyses of the amide I region developed by Williams (1983, 1986). A least-squares fit was made to the Raman profile from 1630 to 1700 cm^{-1} with the reference spectra from 15 proteins with known structures. The reference spectra and programs were provided by R. Williams, USUHS, Bethesda, MD.

Three adjustments were required prior to application of the analysis method (Williams, 1983, 1986). First, side-chain bands that contribute to the low-frequency envelope of the amide I region were subtracted. This was done with a nonlinear least-squares curve fitting program (Wartell & Harrell, 1986). The amide I region was fit with Lorentzian bands representing the side-chain bands below 1630 cm^{-1} and four-five bands representing the amide I modes. The side-chain bands were then subtracted from the spectrum. Second, the water band near 1635 cm^{-1} was subtracted to give a linear background between 1730 and 1800 cm^{-1}, which extrapolated

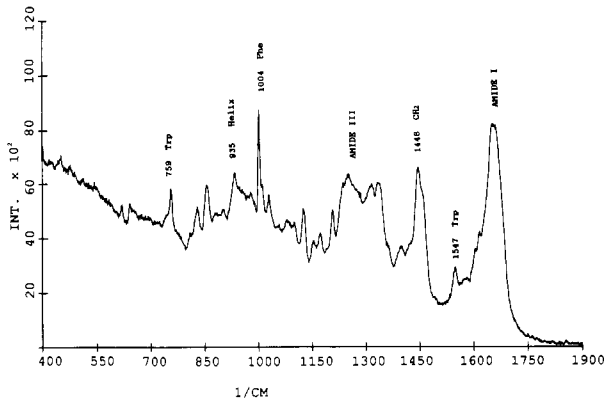

FIGURE 2: Raman spectrum of CRP in 0.2 M NaCl. Several bands and their assignments are indicated.

Table I: Raman Frequencies and Assignments of cAMP Receptor Protein[a]

frequency (cm^{-1})	assignment	frequency (cm^{-1})	assignment
622	Phe	1102	C–N (s), Ala
645	Tyr	1128	C–C (s)
698	amide IV	1156	C–N (s)
741		1174	CH_3 (r)
759	Trp	1208	Tyr, Phe
814		1200–1300	amide III, Tyr
830	Tyr	1316	CH_2 (tw)
857	Tyr	1340	CH_2 (tw)
883	Trp, C–C (s)	1366	Trp, CH
900	C–C (s)	1402	Glu, Asp
935	α-helix	1422	CH_2 (sc), Trp
957	CH_3 sym (r)	1448	CH_2 (sc)
984	Ile	1463	CH_3
1004	Phe	1547	Trp
1014	Trp	1579	Trp
1032	Phe	1604	Phe
1057	C–N	1617	Try, Phe, Trp
1083	C–N (s)	1630–1700	amide I

[a] Assignment codes: (s) stretch; (r) rock; (tw) twist; (sc) scissor. Based on Tu (1986), Thomas (1986), and Otto et al. (1987) and references cited therein.

to the base line around 1500 cm^{-1}. Finally, the frequencies of our data were calibrated by comparing the published spectra of lysozyme and a water sample (Williams, 1986) to our spectra of these samples. The spectra obtained with our instrumentation had to be shifted 2 cm^{-1} higher to match the published spectra. Some frequency shift was anticipated since the reference spectra are 1.7 cm^{-1} higher than they should be for a correctly calibrated spectrometer (Williams, 1986).

Results

Spectra of CRP in Solution. Raman spectra of CRP were obtained in several solvents. In 0.2 M NaCl the CRP spectrum contained no background bands except for the water band near 1635 cm^{-1} (Figure 2). CRP diluted from this sample maintained its activity for site-specific DNA binding in the presence of added cAMP (DeGrazia et al., 1985). The assignments of several Raman bands are shown in Figure 2. Band assignments throughout the spectrum are listed in Table I. At the high concentrations employed, CRP forms multimeric complexes (Ghosaini et al., 1988). We examined the potential effects of aggregation on CRP conformation by examining the spectra from samples at protein concentrations of 5–30 mg/mL. No significant differences were observed (not shown).

The secondary structure content of CRP was estimated from analysis of the amide I region (Williams, 1983, 1986). This analysis assumes four categories of secondary structure; α-helix, β-strand, reverse turn, and undefined or random coil.

Table II: Secondary Structure Evaluation of CRP and Other Proteins by Raman Amide I Analyses

protein	method[a]	% α-helix	% β-strand	% turn	% undefined
lysozyme					
solution	SVA	46	22	19	13
	NNLS	44	23	21	12
crystal	SVA	47	22	18	13
	NNLS	44	22	22	12
	X-ray[b]	46	19	22	12
	Raman[b]	49	19	17	13
ribonuclease (solution and crystal)	SVA	19	48	21	12
	NNLS	20	48	20	11
	X-ray[b]	23	46	21	10
	Raman[b]	23	47	19	12
CRP (0.2 M NaCl)	SVA	43	29	17	11
	NNLS	45	28	17	10

[a] SVA is singular value analysis method of least squares, and NNLS is nonnegative least-squares method, described by Williams (1983, 1986). [b] From previous Raman amide I analyses and X-ray data (Williams, 1983).

Analysis of CRP yielded a secondary structure distribution of 44% α-helix, 28% β strand, 18% turn, and 10% random coil. Since the analysis method is sensitive to background subtraction and frequency calibration, Raman spectra of lysozyme and ribonuclease were examined as controls. Both control proteins gave secondary structure values within 3% of previous Raman and X-ray studies (Table II). The difference between the Raman-derived and X-ray-derived secondary structure content of 15 proteins has a standard deviation of 2–4.5% for each of the four categories (Williams, 1986).

Earlier work indicated that a high-intensity Raman band at 880 cm^{-1} and a sharp well-resolved band at 1359 cm^{-1} result from tryptophan residues located in a hydrophobic environment (Harada & Takeuchi, 1986; Kitagawa, 1979). Neither of these bands was observed in the CRP spectra, indicating that CRP tryptophan residues do not occupy hydrophobic environments. This result is consistent with the CRP–cAMP cocrystal structure in which tryptophan residues are at or near the surface of the protein (see Figure 1).

Siamwiza et al. (1975) has shown that the Raman intensity ratio I_{855}/I_{830} is diagnostic of three different H-bonding states of the *p*-hydroxyl group of tyrosines. A high ratio (2.5) indicates that the hydroxyl group is the acceptor of a strong hydrogen bond from a positive donor group. A low ratio (0.3) indicates that the hydroxyl group is the donor of a strong hydrogen bond to a negative acceptor group, e.g., carboxylate or phosphate anions. When the ratio is between the two extremes, the hydroxyl group functions as both donor and acceptor for moderately strong hydrogen bonds such as solvent water. The measured intensity ratio for CRP was 1.4. This value is an average over the 12 tyrosines per CRP dimer. The crystalline CRP–cAMP complex has four tyrosines that can form internal H-bonds: two are donor/acceptors, and two act as strong donors (I. Weber, personal communication). If the remaining tyrosines are assumed to bind to water, the measured ratio is reasonable for this or a similar structure. The large number of tyrosines in CRP reduces the potential usefulness of these bands.

Small pH changes are known to affect the DNA binding characteristics of CRP. CRP exhibits strong nonspecific binding to both single-stranded and duplex DNA independent of cAMP at pH 6 but not pH 8 (Krakow & Pastan, 1973). To examine the influence of solution pH on CRP conformation, Raman spectra were obtained from CRP dissolved in 30 mM sodium phosphate and 0.15 M NaCl, pH 6, or in 30 mM sodium phosphate and 0.15 M NaCl, pH 8, as well as in 0.2

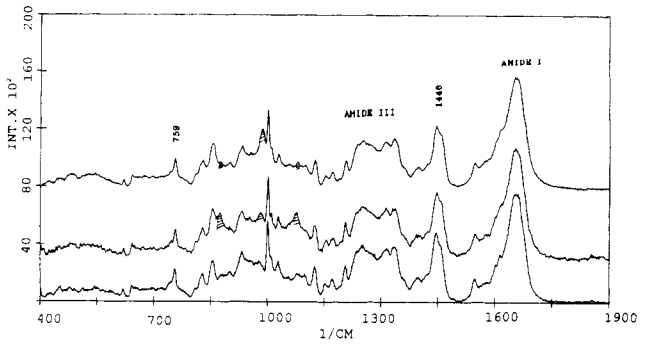

FIGURE 3: Raman spectra of CRP in different solution environments: (bottom) 0.2 M NaCl; (middle) 30 mM NaH_2PO_4, pH 6; (top) 30 mM NaH_2PO_4, pH 8. Sloping background curves were subtracted and the spectra scaled to the 1448-cm^{-1} band. The crosshatched peaks locate phosphate Raman bands.

Table III: Secondary Structure Evaluation of CRP in Different Environments

protein and environment	method	% α-helix	% β-strand	% turn	% undefined
CRP					
soln, pH 6	SVA	43	29	18	10
	NNLS	43	29	18	10
soln, pH 8	SVA	45	28	17	10
	NNLS	45	27	18	10
CRP–cAMP crystal	SVA	37	33	18	12
	NNLS	37	33	18	12
	X-ray[a]	37	36		

[a] From Weber and Steitz (1987).

M NaCl (Figure 3). The broad sloping backgrounds of these spectra were subtracted to simplify the comparison. No significant differences in the CRP Raman spectra were observed aside from those contributed by solvent phosphate. Prominent phosphate peaks are indicated by the crosshatched areas. The Raman spectrum of 30 mM phosphate, pH 8, showed a peak at 985 cm^{-1} and much smaller broad bands at 854 and 520 cm^{-1}. At pH 6 the phosphate solvent produced peaks of similar intensity at 873, 984, and 1072 cm^{-1} and small broad peaks at 853 and 942 cm^{-1}. The amide III region from 1220 to 1300 cm^{-1}, a region known to be sensitive to protein secondary structure, was the same for the three spectra. Quantitative analyses of the amide I region of each spectrum yielded very similar secondary structure distributions (Tables II and III).

Raman Spectrum of CRP–cAMP Crystals. A direct comparison of CRP with and without cAMP in solution was attempted; however, CRP–cAMP complexes precipitated out of solution at the protein concentrations required for Raman spectroscopy. Spectra of CRP–cAMP complexes were obtained from randomly oriented microcrystals immersed in aqueous crystallization medium. Figure 4 shows spectra obtained from CRP–cAMP cocrystals and their aqueous medium. In order to compare the CRP–cAMP cocrystal and CRP solution spectrum, it was necessary to account for and subtract background bands. Aside from the water band near 1635 cm^{-1}, the aqueous medium has only one substantive band at 984 cm^{-1} due to solvent phosphate. The contribution of cAMP to the spectrum was examined by obtaining spectra from both cAMP and CRP solutions under identical light scattering conditions. At the 2:1 cAMP:CRP molar ratio of the CRP–cAMP cocrystals the largest cAMP peaks at 730 and 1340 cm^{-1} were about 5–10% of medium peaks in the CRP spectrum (not shown). This result suggests that cAMP does not contribute significantly to the CRP–cAMP cocrystal spectrum.

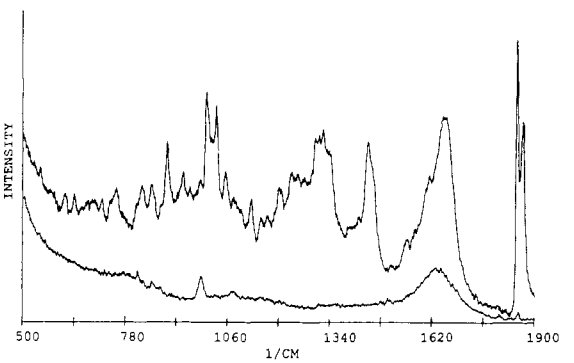

FIGURE 4: Raman spectrum from CRP–cAMP crystals is shown along with a spectrum of the crystal's aqueous medium.

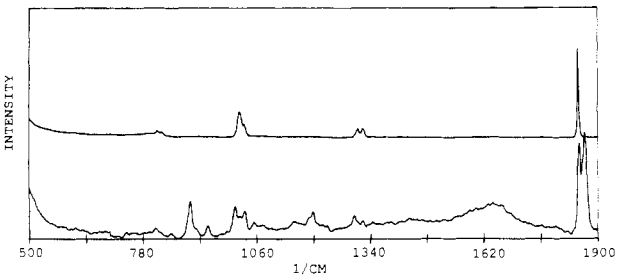

FIGURE 5: Raman spectrum of two glass samples. The top spectrum is from the external surface of a capillary tube. The lower spectrum is from crushed glass situated in a capillary tube. Power levels were similar to that used for the CRP–cAMP crystals.

A complication originating from secondary light scattering was observed. Figure 4 shows that the CRP–cAMP spectrum contains two sharp overlapping peaks at 1856 and 1871 cm^{-1}. These bands are not observed in protein solution spectra. When the laser beam was translated from the surface of the CRP–cAMP cocrystals to the aqueous medium, the intensities of these peaks were drastically reduced (see Figure 4). This observation suggested that these bands—and possibly others—result from a scattering process unrelated to protein or solvent Raman modes. The spectrum of the aqueous medium alone gives the deceptive impression that interfering bands were not significant.

Figure 5 shows spectra obtained by scattering the laser beam from a capillary tube surface and from pieces of crushed tube glass similar in size to the protein crystals and immersed in aqueous medium. Both glass samples produced peaks in the 1860-cm^{-1} region with intensities similar to those observed from the protein crystals. Neither sample produced the same relative intensities of the two peaks seen in the protein spectrum. Scattering the laser beam from a metal surface also produced a doublet peak at these frequencies. The anomalous peaks in the 1860-cm^{-1} region were also observed in the Raman spectrum of lysozyme crystals (not shown). These observations suggest that the peaks are due to the scattering of the strongly reflected Rayleigh light from periodic imperfections in the diffraction gratings, or "diffraction ghosts" (Yager & Gaber, 1987). The occurrence of these bands creates uncertainty in the background of the crystalline CRP–cAMP spectrum. No interference—aside from the water Raman band—was observed in the amide I region. Parts of the protein spectrum from 700 to 1350 cm^{-1} were compromised.

Figure 6 compares the spectrum of CRP in solution with the crystalline CRP–cAMP spectrum after normalization of Raman intensities to the 1448-cm^{-1} band (CH_2 scissor mode). The crushed-glass Raman spectrum was used as a model for the background. It was normalized to the 1871-cm^{-1} peak observed in the CRP–cAMP spectrum. The crushed-glass

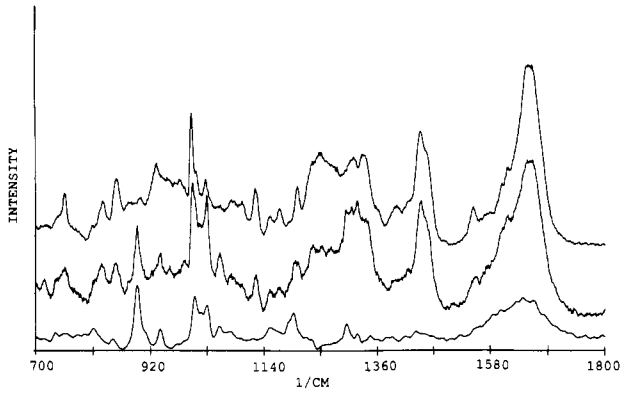

FIGURE 6: Comparison of Raman spectrum of CRP in 0.2 M NaCl solution (top) with spectrum of CRP–cAMP crystals (middle). These two are scaled to the intensity of the 1448-cm^{-1} band. Sloping backgrounds were subtracted. The bottom spectrum is from the crushed-glass sample. It was scaled to the intensity of the 1871-cm^{-1} peak of the CRP–cAMP spectrum (see Figures 4 and 5).

spectrum can account for part or all of the differences between the two protein spectra at 900, 960–1040, and 1190 cm^{-1}. Not all of the spectral differences that exist between CRP and crystalline CRP–cAMP can be attributed to anomalous background bands. The amide III regions of the protein spectra show significant differences. While background bands from 1280 to 1340 cm^{-1} may contribute to the CRP–cAMP spectrum, they cannot account for the decreased intensity centered at 1260 cm^{-1} in the CRP–cAMP spectrum relative to the CRP spectrum. This change was not observed in comparing lysozyme in solution with lysozyme crystals (DeGrazia, 1988). Similarly, the band at 935 cm^{-1} has a decreased intensity in the CRP–cAMP cocrystal spectrum compared to the solution spectrum of CRP. This band is sensitive to the α-helix content of a protein (Tu, 1986; Thomas, 1986). In addition to these differences, small differences were noted in the intensities and frequencies of other bands such as the side-chain bands at 1400 and 1550 cm^{-1}.

The secondary structure distribution of CRP–cAMP cocrystals evaluated from the amide I region was 37% α-helix, 33% β-strand, 18% turn, and 10% undefined (Table III). This result is in good agreement with the X-ray crystallographic values of 37% α-helix and 36% β-strand (Weber & Steitz, 1987) and differs from the estimated secondary structure distribution of CRP in solution. Figure 7 compares the amide I bands of solid versus solution forms of ribonuclease, lysozyme, and CRP after normalization of the spectra for secondary structure analyses. The normalized amide I bands of CRP at pH 6 and pH 8 are also shown.

Discussion

Binding of small ligands leads to conformational changes in the structure of many proteins. Detailed studies on a few allosteric proteins indicate that ligand-induced changes at subunit interfaces are important for mediating quaternary and tertiary structural changes (Stryer, 1988). Ligand binding may rearrange existing secondary structural units or alter the nature of secondary structural units.

Previous studies that employed Raman spectroscopy to measure protein secondary structure have detected a loss of α-helix content in nucleosomes upon binding DNA (Hayashi et al., 1986), a decrease in α-helix content in the gp32 protein of bacteriophage T4 upon binding oligonucleotides (Otto et al., 1987a,b), and an increased α-helix content accompanied by a corresponding decrease in β-strand content upon binding Ca^{2+} to calmodulin (Hildebrant et al., 1987; Follenius et al., 1987; Hodges, 1987).

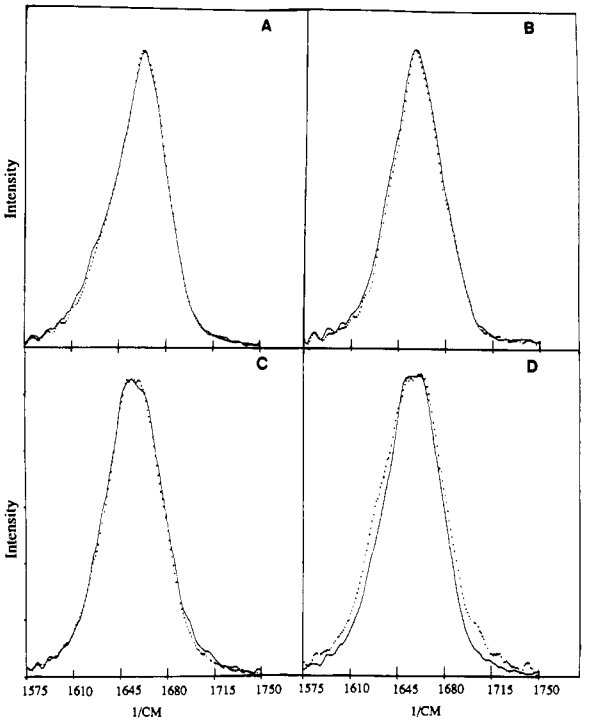

FIGURE 7: Raman spectra of amide I region of proteins examined. Side-chain and water bands were subtracted. For panels A, B, and D, the line corresponds to a solution spectrum and the dots correspond to a crystal spectrum. (A) Ribonuclease; (B) lysozyme; (C) CRP at pH 6 (dots) and pH 8 (line); (D) CRP in solution vs CRP–cAMP crystal.

The Raman data reported in this study suggest that differences exist between the secondary structures of crystalline CRP–cAMP and CRP in solution. This conclusion is based on several observations that are individually subject to other interpretations but in concert support this notion. The amide III region of the two forms of CRP shows differences indicating an alteration in secondary structure and/or changes to residues that contribute to this region. Amide I analyses indicate that CRP has 7% more α-helix and 5% less β-strand than the CRP–cAMP complex. These differences are close to the error limits of the estimation procedure and cannot by themselves be regarded as highly accurate. However, the differences were reproducible, and the secondary structure distribution of crystalline CRP–cAMP agrees with that made from X-ray analysis. The fact that similar differences between the spectra of crystalline lysozyme and lysozyme in solution were not observed also suggests that the differences in the CRP forms are not experimental artifacts (Table II). Finally, the enhanced intensity at 935 cm^{-1} for CRP relative to CRP–cAMP cocrystals is consistent with an increased α-helix content in CRP.

Recent studies by Hyduk and Lee (1989) indicate that three different CRP conformations exist for free CRP, CRP bound by one cAMP, and CRP with two bound cAMP molecules. The current Raman study supports the contention that CRP alone and CRP with two bound cAMP have different conformations.

The Raman spectrum of CRP in solution buffered at pH 6, which supports strong *nonspecific* CRP binding to DNA in the absence of cAMP, was virtually identical with that of CRP in a pH 8 solvent (Figure 3). This result indicates that pH-mediated effects on CRP binding to DNA do not induce large changes in CRP secondary structure and are most likely due to localized changes in protein charge. CRP has an isoelectric point of 9.2 (Zubay et al., 1970).

Alternative interpretations of the Raman data were considered. The observed differences between CRP in solution and CRP in the CRP–cAMP cocrystals could be due to an unequal distribution of inactive CRP in the two samples. Data presented by Fried and Crothers (1983) suggested that CRP–cAMP crystals may involve a form of CRP that has high activity in site-specific DNA binding. We were unable to reproduce this observation. The DNA binding activity of our redissolved CRP–cAMP cocrystals was similar to that of the initial CRP preparation. In a different test of this hypothesis, the Raman spectrum of inactive CRP was analyzed. CRP that had precipitated during the concentration steps had negligible site-specific DNA binding activity in the presence of cAMP and at a 4:1 CRP:DNA molar ratio. This form of CRP had a secondary structure distribution of 33% α-helix, 33% β-strand, 20% turn, and 14% undefined (not shown). This preliminary observation indicates that inactive CRP contains less rather than more α-helix content than native CRP. It does not support that notion that the differences between the CRP–cAMP cocrystals and CRP in solution are attributable to inactive CRP.

Small distributed differences in peptide backbone angles and/or hydrogen bonding between the CRP–cAMP crystal and CRP in solution could influence the Raman bands. This possibility cannot be ruled out.

ACKNOWLEDGMENTS

We are indebted to Dr. Robert W. Williams (USUHS) for providing the secondary structure analysis programs and help in their implementation. We thank James Cagle for help in keeping the instrumentation functional and Jane Clark for her help with the computer graphics of CRP. We also thank Patrick Kelly for discussions.

REFERENCES

Adhya, S., & Garges, S. (1982) *Cell 29*, 287.
Aiba, H., Fujimoto, S., & Ozaki, N. (1982) *Nucleic Acids Res. 10*, 1345.
Aiba, H., Nakamura, T., Mitani, H., & Mori, H. (1985) *EMBO J. 4*, 3329.
Anderson, W. B., Schneider, A. B., Emmer, M., Perlaman, R. L., & Pastan, I. (1971) *J. Biol. Chem. 246*, 5929.
Cossart, P., & Gicquel-Sanzey, B. (1982) *Nucleic Acids Res. 10*, 1363.
de Crombugghe, B., Busby, S., & Buc, H. (1984) *Science 224*, 831.
DeGrazia, H. (1988) Ph.D. Thesis, Georgia Institute of Technology.
DeGrazia, H., Abhiraman, S., & Wartell, R. M. (1985) *Nucleic Acids Res. 13*, 7483.
Dessen, A., Schwartz, M., & Ullmann, A. (1978) *Mol. Gen. Genet. 162*, 83.
Eilen, E., & Krakow, J. (1977) *J. Mol. Biol. 114*, 47.
Eilen, E., Pampeno, C., & Krakow, J. (1978) *Biochemistry 17*, 2469.
Follenius, A., Berjot, M., Angiboust, J.-F., Gerard, D., & Manfait, M. (1987) *Recl. Trav. Chim. Pays-Bas 106*, 175.
Fried, M. G., & Crothers, D. M. (1981) *Nucleic Acids Res. 9*, 6505.
Fried, M. G., & Crothers, D. M. (1983) *Nucleic Acids Res. 11*, 141.
Garges, S., & Adhya, S. (1985) *Cell 41*, 745.
Garner, M. M., & Revzin, A. (1981) *Nucleic Acids Res. 9*, 2945.
Ghosaini, L. R., Brown, A. M., & Sturtevant, J. M. (1988) *Biochemistry 27*, 5257.
Harada, I., & Takeuchi, H. (1986) in *Spectroscopy of Biological Systems* (Clark, R. J. H., & Hester, R. E., Eds.) p 113, Wiley, New York.
Harman, J. G., & Dobrogosz, W. J. (1983) *J. Bacteriol. 153*, 191.
Harman, J. G., McKenney, K., & Peterkofsky, A. (1986) *J. Biol. Chem. 261*, 16332.
Harman, J. G., Peterkofsky, A., & McKenney, K. (1988) *J. Biol. Chem. 263*, 8072.
Hayashi, H., Nishimura, Y., Datahira, M., & Tsuboi, M. (1986) *Nucleic Acid Res. 14*, 2583.
Heyduk, T., & Lee, J. C. (1989) *Biochemistry 28*, 6914.
Hildebrant, P., Copeland, R. A., Spiro, T. G., & Pendergast, F. G. (1987) *Recl. Trav. Chim. Pays-Bas 106*, 264.
Hodges, R. S. (1987) *Recl. Trav. Chim. Pays-Bas 106*, 263.
Kitagawa, T., Azuma, T., & Hamaguchi, K. (1979) *Biopolymers 18*, 451.
Krakow, J. S., & Pastan, I. (1973) *Proc. Natl. Acad. Sci. U.S.A. 70*, 2429.
Kumar, S. S., Murthy, N. S., & Krakow, J. (1980) *FEBS Lett. 109*, 121.
Kypr, J., & Mrazek, J. (1985) *Biochem. Biophys. Res. Commun. 131*, 780.
McKay, D. B., & Steitz, T. A. (1981) *Nature 290*, 744.
McKay, D. B., Weber, I. T., & Steitz, T. A. (1982) *J. Biol. Chem. 257*, 9518.
Otto, C., de Mul, F. F. M., Harmsen, B. J. M., & Greve, J. (1987a) *Nucleic Acid Res. 15*, 7605.
Otto, C., de Mul, F. F. M., & Greve, J. (1987b) *Biopolymers 26*, 1667.
Pampeno, C., & Krakow, J. (1979) *Biochemistry 18*, 1519.
Rosenblatt, M., Beaudetti, N. V., & Fasman, G. D. (1980) *Proc. Natl. Acad. Sci. U.S.A. 77*, 3983.
Siamwiza, M. N., Lord, R. C., Chen, M. C., Takmatsu, T., Harada, I., Matsuura, H., & Shimanouchi, T. (1975) *Biochemistry 14*, 4870.
Stryer, L. (1988) in *Biochemistry*, W. H. Freeman, New York
Thomas, G. J., Jr. (1986) *Adv. Spectrosc. 13*, 233.
Tu, A. T. (1986) in *Spectroscopy of Biological Systems* (Clark, R. J. H., & Hester, R. E., Eds.) p 47, Wiley, New York.
Ullmann, A., & Danchin, A. (1983) *Adv. Cyclic Nucleotide Res. 15*, 1.
Wartell, R. M., & Harrell, J. T. (1986) *Biochemistry 25*, 2664.
Weber, I. T., & Steitz, T. A. (1987) *J. Biol. Chem. 198*, 311.
Williams, R. W. (1983) *J. Mol. Biol. 166*, 581.
Williams, R. W. (1986) *Methods Enzymol. 130*, 311.
Williams, R. W., & Teeter, M. M. (1984) *Biochemistry 23*, 6796.
Wu, C.-W., & Wu, F. (1974) *Biochemistry 13*, 2573.
Wu, F., Nath, K., & Wu, C.-W. (1974) *Biochemistry 13*, 2567.
Yager, P., & Gaber, B. P. (1987) in *Biological Applications of Raman Spectroscopy* (Spiro, T. G., Ed.) p 214, Wiley, New York.
Zubay, B., Schwartz, D., & Beckwith, J. (1970) *Proc. Natl. Acad. Sci. U.S.A. 66*, 104.